Modeling and simulation of a fluidized bed gasifier

Jain, A. A., Mehra, A., & Ranade, V. V. (2018). Modeling and simulation of a fluidized bed gasifier. *Asia-Pacific Journal of Chemical Engineering*, *13*(1), [e2155]. https://doi.org/10.1002/apj.2155

Published in:
Asia-Pacific Journal of Chemical Engineering

Document Version:
Peer reviewed version

Modeling and Simulation of a Fluidized Bed Gasifier

A .A. Jain[1, 2], A. Mehra[1] and V .V. Ranade[2,*]

[1] Department of Chemical Engineering, Indian Institute of Technology, Bombay, Powai, INDIA 400076

[2] Industrial flow modeling group, National Chemical Laboratory, Pune, INDIA 411008

Abstract

A mathematical model to simulate continuous gasification of coal particles in a bubbling fluidized bed reactor (FBR) is presented. Material and energy balance equations have been formulated based on the two phase theory. Well known correlations have been used to estimate the hydrodynamics. Devolatilization, heterogeneous reactions and homogenous reactions have been included in the model. The model is used to simulate twenty nine experimental data sets from the published literature. The model predictions agree very well with the experimental data by adjusting the particle size. After establishing agreement with the data, the model was used to investigate influence of various operating parameters on overall performance (carbon conversion and the gross calorific value of generated gas). Thermodynamic analysis (using the minimization of the Gibbs free energy approach) has also been discussed. The presented model and results provide useful tool and insight on design and operation of fluidized bed gasifier.

Keywords: Fluidized bed, gasification, two phase, model

---

*Corresponding author; Current address: School of Chemistry and Chemical Engineering, Queen's University Belfast, Belfast, UK. Email: V.Ranade@qub.ac.uk

1. Introduction

India boasts of 7.1 % of world's total coal reserve [1], 70 % of the total power generated in India is from coal-fired power plants [2]. As reported by various organizations [3–5], India faces around 10-13 % deficit in terms of energy supply to demand. With its relatively comfortable resource base compared to limited known oil & gas resources; coal is the obvious, affordable and sustainable choice for generation of electricity. Therefore, India's power development programme is heavily dependent on coal and its quality is an important parameter that influences the performance of the power stations. Conventional technologies based on the coal combustion process are low on efficiency and release green house gases such as carbon dioxide, sulphur dioxide and nitrogen oxides. Looking at the scenario where high demand of energy is forecasted [6], it is essential that India looks toward other technologies also termed as clean coal technologies [7,8]. Thereby, development of means to convert coal from its native form into useful gases and liquids in ways that are energy efficient, non-polluting and economical is key in fulfilling the needs of our society [9]. Coal gasification has been regarded internationally as an effective way for clean use of coal especially for the production of energy and also production of synthetic chemicals [10] .

Research and development on gasification with high ash coal (Indian coal) needs to be a priority area. There are various technologies developed and used worldwide for coal gasification including moving bed , fluidized bed (bubbling and circulating fluidized bed) and entrained bed gasifier being the prominent ones [11] .Among this moving bed and the fluidized bed are considered more apt for handling high ash coal [12]. Fluidized bed has certain advantages over moving bed i.e. scaling and environmental issues. Moving bed gasifier generate tarry products whereas fluidized bed gasifier yield only gaseous product as the volatiles get cracked up facilitating more environment friendly products and also easier plant operation [13] .The other advantages of fluidized bed gasifier are well documented [14] i.e. good gas solid contact, excellent heat transfer characteristics, better temperature control, large heat storage capacity, good degree of turbulence and high volumetric capacity. Mathematical models are efficient tool to allow quantitative representation of the physical processes occurring and also are useful in the designing, optimization and control of processes. In this work we have developed a mathematical model for the gasification of high ash Indian coal.

Modeling of biomass gasification [15,16] and coal gasification [17] in fluidized bed has been reviewed recently. Modeling of fluidized bed can be segregated into three approaches; Thermodynamic models (See **Table 1a**), data driven models [18] and rate based models. Rate based models are of further two types i.e. chemical reaction engineering models (CRE) (see **Table 1b**) in which the momentum equations are not explicitly solved (instead semi empirical correlations are used to describe the gas solid hydrodynamics) and Computational Fluid Dynamic (CFD) models [19–22] in which the momentum equations are explicitly solved but are computational very expensive [15]. Thermodynamic models do not take into account the chemical reactions or the hydrodynamics into consideration but calculates the equilibrium composition of a system at a particular operating condition by minimizing the Gibbs free energy. The previous attempts to model the fluidized bed gasifier have been listed in **Table 1a-b**. It can be inferred from **Table 1a** that thermodynamic models or modified thermodynamic models show good match with experimental data for biomass/coal gasification in downdraft, entrained bed and fluidized bed gasifiers. Various authors [23,24] have used the quasi equilibrium temperature i.e. the equilibrium of the reactions defined in the model are evaluated at the temperature which is lower than the actual process temperature while some authors [25–30] have used coefficients for correcting the equilibrium constants of the water gas shift and the methane reaction for better comparison with experimental data. There have been attempts [25,31] for coal gasification wherein the input of carbon to the model is equal to the actual carbon conversion reported and the same showed good match to the experimental data. Thermodynamic models give a fair idea into the limits of operation and also the qualitative change in the outlet gas composition and generation rate with change in various operating parameters [17].

CRE models are formulated on the first principles of conservation of mass and energy balance, in these models the gas-solid hydrodynamics (by use semi-empirical correlations) and complex chemical reactions are taken account of; hence are more realistic. Table 1b lists the review of previous works in CRE modeling of FBG.

Table 1a: Review of previous works in thermodynamic analysis of coal gasification

Table 1b: Review of previous CRE models

Unlike most previous works where one dimensional steady state model of FBG has been presented, in this work we have proposed a transient model which can be useful to study start-

up, shut down and pressure build up phenomena in FBG. We have also included a detailed elemental balance approach to calculate the fractions of gases released from coal devolatilization instead of assuming a correlation [32,33]. Most previous models have modeled the emulsion phase gas as a continuously stirred tank reactor (CSTR) or a plug flow reactor (PFR) and the bubble phase as a PFR. In this study we have modeled the bubble phase gas as a series of mixing cells wherein the number of CSTR is a modeling parameter. A comparison studies wherein the effect of mixing of gas in bubble phase has been done by varying the number of mixing cells. A thermodynamic analysis of coal gasification was done using process simulator Aspen Plus. An exhaustive set of 29 experimental data reported[34] for two different types of coal were simulated with the developed models. A comparison between the CRE model and the thermodynamic analysis has been done in order to understand the role of gas-solid hydrodynamics and the chemical reactions in the gasifier. Such a comparison has not been previously been reported. We have further used the model to carry out sensitivity analysis with respect to various parameters such as feed composition (air and steam) and coal feed rate**.** This work shall serve us a step towards developing a mixing cell framework [35].

2. Thermodynamic Model

Thermodynamic analysis of gasification can be carried by two methods viz. stoichiometric [36] and non-stoichiometric approach [37]. In this work we have used the latter approach using the RGIBBS module of the process simulator Aspen Plus [38] . The schematic representation of the model developed in Aspen plus can be seen in **Figure 1**. A Splitter module was used in the model to control the carbon input to the RGIBBS module. Two sets of simulations for each experimental dataset were carried out. In one simulation the carbon inlet to the RGIBBS module was set equal to carbon content of coal (as per ultimate analysis) while in the second set it was set equal to the carbon conversion reported in the experimental results. First, the model implementation was verified by reproducing the published results[38].

Figure 1: Schematic representation of the thermodynamic model in Aspen Plus

3. CRE Model

A generalized mathematical model of coal gasification in a fluidized bed, incorporating mass and energy balances, coal devolatilization and chemical processes, is presented. A schematic representation of the model is shown in **Figure 2.** Coal is continuously entered into the reactor and it reacts with steam and oxygen to produce synthetic gases composed mostly of carbon monoxide and hydrogen apart from carbon dioxide and methane. The hydrodynamic behavior of the fluidized bed is described by the two phase theory of fluidization. The freeboard region is represented as a vapor phase; it consists of the gases exiting out of the emulsion and bubble phases.

Figure 2: CRE Model for a fluidized bed gasifier reactor

Assumptions:

1. Emulsion phase consisting of solids and the gases required to maintain the solids at U_{MF}.
2. The bubbles are assumed to be of uniform size in a cell. The gases in the bubble phase consists of the extra gases i.e. U_g - U_{mf} in the inlet feed and also consists of the gases entering from the emulsion phase (the extra amount of gases produced due to the heterogeneous reactions i.e. char reaction and devolatilization). Bubble phase is modeled as a series of mixing cells.
3. The Heterogeneous reactions are assumed to take place only in the emulsion phase while gas-gas reactions are assumed to occur in all the phases i.e. emulsion, bubble and vapour.
4. Emulsion phase gas and solids are modeled as a CSTR to take into account back mixing due to the movement of solids in the bed.
5. Vapour phase is also modeled as a CSTR.
6. Devolatilization reactions are assumed to occur instantaneously on entry to the bed and produces volatiles and char in the emulsion phase, the fractions of the gases are found by elemental balance. Volatiles are assumed to be uniformly distributed in the emulsion phase considering that the solids are well mixed. The amount of heat liberated during devolatilization reaction is neglected.

7. The emulsion and the bubble phase are linked to each other by convection and inter phase mass and heat transfer term.
8. The solids are assumed to be uniform in size and spherical in shape.

3.1 CRE Model Equations

The mathematical model consists of overall mass balance for the phases, mass balance equations written for each species and energy balance for different phases for the reactor. The approach and the detailed equations have been included in APPENDIX A.

To model the fluid dynamics in the fluidized bed; empirical/semi-empirical correlations have been employed. These correlations describe the important dynamics of the bubbles, Bubbles play an important role in the gas solid flows occurring inside the fluidized bed, and they are responsible for the movement of the solids. Thereby, the role of bubble velocity, bubble diameter and the bubble voidage in the system play an important role in the overall performance of the gasifier. Various correlations were reviewed to calculate the bubble diameter, bubble voidage, bubble velocity and mass transfer coefficient. The set of correlations used in the model has been listed in **Table 2.**

Table 2: List of correlations used in this model

3.2 Chemical Reactions

There are several homogenous and heterogeneous reactions occurring in the gasifier. In this work we have assumed the set of reactions assumed to occur in the reactor are as follows:

Heterogeneous reactions

$$CH_xO_y(VM) \rightarrow x_1CH_4 + x_2CO + + x_3CO_2 + x_4H_2 + x_5H_2O + C_s \qquad R_1$$

$$C_s + O_2 \rightarrow CO_2 \qquad R_2$$

$$C_s + CO_2 \rightarrow 2CO \qquad R_3$$

$$C_s + H_2O \rightarrow CO + H_2 \qquad R_4$$

$C_s + 2H_2 \rightarrow CH_4$ R_5

Homogenous reactions

$CO + H_2O \rightarrow CO_2 + H_2$ R_5

$CO_2 + H_2 \rightarrow CO + H_2O$ R_6

$CO + \frac{1}{2}O_2 \rightarrow CO_2$ R_7

$H_2 + \frac{1}{2}O_2 \rightarrow H_2O$ R_8

$CH_4 + 2O_2 \rightarrow CO_2 + 2H_2O$ R_9

The prediction of volatilized components (R_1) from coal is difficult not only due to its versatile nature but also due to the fact that it depends on number of factors , including heating rate , pressure, particle size and temperature [39]. Few studies have considered using correlations to find the fraction of gases released during this reaction [33,40], while few have considered elemental balance (linking the same to the Ultimate and Proximate Analysis) to find the fractions of gases released from the devolatilization step. Kaushal et al.[41] have considered the elemental balance and also have considered the amount of char produced as a modeling parameter. In this model, we have considered the elemental balance approach[39,42] to find the fractions of gases released and considered the fixed carbon released as the amount of char released during the devolatilization of coal. Regarding the kinetics of the reaction there are two approaches, one is to assume the kinetics reported in literature or assume that devolatilization occurs instantaneously. Considering the fact that the devolatilization occurs much faster than the gasification reactions and also that the reactor is operating at a very high temperature (1100-1200 K), devolatilization has been assumed instantaneous [33]. The distribution of the devolatilized gases is distributed evenly across the emulsion phase. The rate expression for the heterogeneous and the homogenous reactions taken from literature has been listed in **Table 3.**

Table 3**: Reaction rate expression for the heterogeneous and homogenous reactions**

The program consists of different modules i.e. kinetics, energy equation and mass balance equations. Seven algebraic equations, ten differential equations in emulsion phase and 7 differential equations for each bubble and vapor phase to be solved in the model; ode15s solver of Matlab^{TM} has been used to solve the set of equations. ode15s [43] solves stiff differential equations and DAE. The default tolerances i.e. relative tolerance at 1e-03 and the absolute tolerances i.e. 1e-06 have been used. The tolerances have been varied to the tune of 1e-13; the same did not yield any difference in the solution.

4. Results and discussion

The simulation results of the thermodynamic and CRE models described in the above section are discussed in this section. The input to the model is based on the findings of the experiments conducted (in a bubbling fluidized bed of diameter 0.2 m) with high ash Indian coal at CIMFR, Dhanbad [34]. 18 experiments conducted with Rajmahal coal and the 11 experimental data reported with North Karanpura (NK) coal reported in the paper were used as inputs for this model. The input details and the proximate and ultimate analysis of the coal can be found in **Table 1-2** in Chavan et al. (2012) (see Supporting Information **Table S1a-b).** The performance of the gasification process is described in terms of two macroscopic parameters i.e. cold gas efficiency and the carbon conversion (**Eq. 1 and 2**) [33]. We have compared the results of the model with those of experimental results in terms of these parameters.

$$\text{Carbon Conversion (X, \%)} = \left(\frac{\text{Flow rate of carbon in - Flow rate of carbon out}}{\text{Flow rate of carbon in}}\right) \text{x } 100 \quad (1)$$

$$\text{Cold gas efficiency (CGE, \%)} = \frac{\text{chemical energy}}{\text{coal energy}} \text{ x } 100 \quad (2)$$

$$\text{Chemical energy} = \text{mass flow (kg/s) x heating value (kcal/kg)} \quad (3)$$

$$\text{Coal energy (MJ/kg)} = 33.855\text{C} + 144.9\text{H} + 18.06\text{O} + 10.5\text{S} \quad [44] \quad (4)$$

4.1 Thermodynamic model

The results from the thermodynamic model developed in Aspen Plus as discussed in Section 2 are shown in **Figure 3a** and **Figure 3b**. It is observed (from **Figure 3a**) that at the operating temperature reported when the carbon input to the model was equal to the carbon content of

coal (as per ultimate analysis), there is 100 % X; CGE calculated were higher than the reported CGE for all the 29 experimental data. A second set of simulations in which the carbon inlet to the model was equal to the carbon conversion reported was carried out. It is seen from Figure 3b that with these simulations for 18 experimental data of Rajmahal Coal CGE is around 40 % lower than the experimental data while for the 11 NK coal the CGE was spread in the range of 10-20%. These results point out the importance of the development of kinetic based model for the fluidized bed gasifier as thermodynamic model is not sufficient to capture the results of the fluidized bed gasifier, though it may be noted that the thermodynamic analysis do show a good match with the qualitative trends of the experimental data with respect to CGE.

Figure 3a: Parity plot comparing the simulation results of 18 experimental data with Rajmahal coal for CGE

Figure 3b: Parity plot comparing the simulation results of 11 experimental data of North Karanpura coal (NK) for CGE

4.2 CRE Model

The effect of number of mixing cell in bubble phase on CGE and X was studied. As can be seen in **Figure 4a** that as number of mixing cells in bubble phase increases it leads to slight increase in carbon conversion and CGE and no effect after mixing cell were more than two. Results showed that the amount of the hydrogen in the product gases very slightly higher as the number of bubble phase increase, this is due to the increase in mass transfer of steam from bubble phase to emulsion phase leading to higher hydro-gasification reaction and hence higher gasification and CGE. The increase in CGE and X being very minor; for further simulations the number of mixing cells for bubble phase was set equal to one.

Figure 4a: Effect of bubble gas mixing on CGE and X

The diameter of particle (d_p) have been reported in the experimental data to be between 0-3 mm, thereby in this model d_p is calculated using the relation as shown in **Equation (5)** wherein d_{po} was used as a modeling parameter.

$$d_p = d_{p_o} \left(\frac{f_{ash} + (1\text{-}X) f_c}{f_{ash} + f_C} \right)^{\frac{1}{3}} \qquad (5)$$

Simulations were carried out for a single experimental dataset by varying the values of dp_o and as can be seen from the **Figure 4b,** as the diameter of particle increase the X and CGE decreases. The d_{po} were varied in order to minimize the objective function as in **Equation (6).** The optimized d_{po} was then used to run for the remaining 17 and 10 experimental data set. The diameter of particle was found optimized at 1.7 mm for 18 experimental data set with Rajmahal coal and 1.5 mm for the 11 experimental data set with NK coal. Using the values of experimental data of f_{ash} and f_C **.** It was found that there was not much variation in dp for the 18 and 11 experimental datasets for the same value of d_{po} .

$$y_{error} = \left(\frac{y_{exp} - y_{sim}}{y_{exp}}\right) \text{ x } 100 \qquad (6)$$

Where y = X and CGE

Figure 4b: Variation in CGE and X with dp

A typical profile of weight fraction of species in emulsion and bubble is shown in **Figure 5a-b**. The profile of vapor phase is similar to the bubble phase. Gases in all three phases obtain pseudo-steady state in few seconds with oxygen being consumed in seconds of gas entering in the reactor, while the solids species take some time a long time (12000 seconds) in obtaining steady state values (see **Figure 5c**). A typical temperature profile is shown in **Figure 5d**. The temperature of the emulsion, bubble and vapor phase are equal while the temperature of solids are slightly higher than the emulsion phase.

Figure 5a: Typical profile of gaseous species in the emulsion phase

Figure 5b: Typical profile of gaseous species in the bubble phase

Figure 5c: Typical profile of species in the solid phase

Figure 5d: Temperature profile for the emulsion, solid and bubble phase

It can be inferred from the **Figure 6a-b** and **Figure 3a-b** that the model results show good match with the experimental results. The improvement in prediction of carbon conversion by the CRE model as compared to thermodynamic model as discussed in Section 4.1 have been compared in **Figure 3a-b**. It may be noted that the carbon conversion is consistently over

predicted while the CGE is under predicted for the 18 experimental data set of RajMahal coal, the same can be further investigated by optimizing the kinetic rate constants but given the condition that the composition of species gases are not reported in these experiments and the fact that the results are in the acceptable range of error, the exercise of changing he kinetic to further fine tune the model to the experimental results is not felt necessary. It can be seen from the **Figures 6a & 6b** that for the NK coal the same is in the expected range of 0-20% for both carbon conversion and CGE**.**

Figure 6a: Parity plot comparing the simulation results of 18 experimental data with Rajmahal coal for carbon conversion

Figure 6b: Parity plot comparing the simulation results of 11 experimental data of North Karanpura coal (NK) for carbon conversion

The steady state bubble voidage is around 0.58-0.60 for most cases which is slightly lesser with the reported value of 0.65 [32] , while the bubble diameter (mean) is around 0.09 m which agrees well with the hypothesis that if the diameter of particle is lower than half the diameter of the reactor than it operates in the bubbling regime [32]. With this validated model, further studies to study the influence of various operating parameters have been carried out. (The steady state values of the model parameters bubble voidage, bubble velocity and the diameter of bubble have been listed in Supporting Information **Table S2a-b)**.

4.3. Influence of operating parameters

Increase in coal feed rate leads to decrease in the carbon conversion and also leads to a decrease in the coal gas efficiency of the gas releasing out of the system (see **Figure 7a**). It is obvious for with increase in the coal feed rate more amount of carbon enters the system for the same amount of oxygen leading to lower carbon conversion and syngas composition in the product gases leading to lower cold gas efficiency.

Figure 7a: Influence of coal feed rate to the carbon conversion and the cold gas efficiency

As the steam feed rate increase the amount of steam increases in the system there is slight increase in the carbon conversion and the cold gas efficiency as shown in **Figure 7b**, this is

due to the fact that as the amount of steam increases, it leads to higher hydro gasification reaction.

Figure 7b: Influence of steam feed rate to the carbon conversion and the cold gas efficiency

It was observed that though the influence of operating parameters to X and CGE is in agreement with the experimental observation [34]. We also carried out the simulation to check the effect of bed temperature and air feed rate on the X and GCV and the results were compared with a different set of experimental setup [45] as shown in **Figure 7c**. It can be observed that as bed temperature increases it lead to higher carbon conversion and GCV and is in good agreement with the reported experimental results. **Figure 7d** shows that as the air feed rate increases the amount of oxygen increases leading to higher carbon conversion and also decrease in the cold gas efficiency. This trend is obvious as with increases in air more particles come in contact with oxygen leading to higher conversion and the syngas viz. CO and H_2 combusting to CO_2 and H_2O leading to lower CGE.

Figure 7c: Influence of bed temperature to the carbon conversion and the GCV

Figure 7d: Influence of air/coal ratio to the carbon conversion and the GCV

5. Summary and Conclusions

Thermodynamic model and CRE models were presented for simulating a fluidized bed coal gasifier. Thermodynamic analysis of coal gasification was done using RGIBBS model of process simulator Aspen Plus. A transient CRE model using the two phase theory which takes into account the hydrodynamics and chemical reactions into consideration was developed. The results of the model were compared with the 29 experimental data [34]. Simulations were carried out for 18 experimental data conducted with Rajmahal coal and 11 experimental data of North Karanpura coal. The key conclusions based on this study are:

- A thermodynamic model was developed using process simulator Aspen Plus. Two sets of simulations for each experimental dataset were carried out. In one simulation the carbon inlet to the RGIBBS module was set equal to carbon content of coal (as per ultimate analysis) while in the second set it was set equal to the carbon conversion

reported in the experimental results. First, the model implementation was verified by reproducing the published results. Both the model showed poor comparison with the CGE as reported in experimental data, the qualitative trends though matched with the experimental observations.

- A transient CRE model was developed based on the two phase theory wherein the emulsion phase was modeled as a perfectly mixed reactor while the bubble phase was modeled as a series of mixing cells. The simulation results of the developed CRE model showed good match with 29 experimental data published in literature.
- Effect of gas mixing in bubble phase was studied by varying the number of mixing cells. It was seen that there was a very slight increase in X and CGE by increasing the number of CSTR's and negligible increase after two cells.
- The developed model was further used to study the influence of operating parameters i.e. Bed temperature, steam , air and coal feed rate It was seen that as steam , air feed rate and bed temperature increases , it lead to higher carbon conversion ,Increase in air and coal feed rate lead to lower CGE. The trends are in agreement with experimental data.

Validation of the model results with further diverse data will be useful for the fine tuning of the model. The developed CRE model is a step towards the development of a mixing cell framework [35] for a fluidized bed gasifier. The developed model provides useful insight into the operations of bubbling fluidized bed. The computational tool can be effectively used for the design and optimization of bubbling fluidized bed.

Acknowledgements

One of the authors (AAJ) thanks the Council of Scientific and Industrial Research (CSIR) for awarding a research fellowship. VVR also would like to thank partial support by the NWP-21 project of CSIR.

Notations

Parameter	Definition	Units
A	cross sectional area of the reactor	m^2
A_s	total surface area of solids exposed to gases for reaction	m^2

$C_{p,j,B}$	specific heat of gases in bubbles	$\frac{kJ}{kmolK}$
$C_{p,j,E}$	specific heat of gases in emulsion	$\frac{kJ}{kmolK}$
$C_{p,S}$	specific heat of solids	$\frac{kJ}{kmolK}$
d_B	diameter of rising bubble	m
d_{BM}	maximum bubble diameter	m
d_{BO}	initial diameter of bubbles	m
D_G	Diffusivity of gas	$\frac{m^2}{sec}$
E_i	activation energy	$\frac{J}{kmol}$
H	height of the reactor (emulsion+bubble)	m
$(-\Delta H)_i$	heat of reaction due to 'I'th reaction	$\frac{J}{kmol}$
h_{BC}	heat transfer coefficient (bubble -cloud)	$\frac{J}{sm^2K}$
h_{BE}	heat transfer coefficient (cloud-emulsion)	$\frac{J}{sm^2K}$
h_{GE-B}	heat transfer coefficient between gas in emulsion to bubble phase	$\frac{J}{sm^2K}$
h_{GE-S}	heat transfer coefficient between gas in emulsion to solids	$\frac{J}{sm^2K}$
H_{max}	maximum height of the reactor	m
k_{BC}	mass transfer coefficient (bubble-cloud)	$\frac{1}{s}$
$k_{be,j}$	mass transfer coefficient for the j 'th' component	$\frac{1}{s}$
k_{CE}	mass transfer coefficient (cloud-emulsion)	$\frac{1}{s}$
k_G	Thermal conductivity of gas	$\frac{J}{smK}$
$k_{o,i}$	pre exponential factor	$\frac{m}{s}$ or $\frac{m^3}{kmols}$
$\dot{m}_{ash}$	inlet mass flow rate of ash in coal particle	$\frac{kg}{s}$
$M_{avg,B}$	average molecular weight of components in the bubble phase	$\frac{kg}{kmol}$
$M_{avg,E}$	average molecular weight of components in the emulsion phase	$\frac{kg}{kmol}$
$M_{avg,V}$	average molecular weight of components in the vapor phase	$\frac{kg}{kmol}$
$\dot{m}_C$	inlet mass flow rate of carbon in coal particle	$\frac{kg}{s}$
$\dot{m}_{G,in}$	inlet mass flow rate of gas at any time 't'	$\frac{kg}{s}$
$\dot{m}_{GB,in}$	inlet mass flow rate of bubble gases	$\frac{kg}{s}$
$\dot{m}_{GB,out}$	outlet mass flow rate of bubble gases	$\frac{kg}{s}$

$\dot{m}_{GE,B}$	mass flow rate of gases from emulsion to bubble	$\frac{kg}{s}$
$\dot{m}_{GE,in}$	inlet mass flow rate of emulsion gases	$\frac{kg}{s}$
$\dot{m}_{GE,out}$	total mass of solids gasified at any time ‘t’	$\frac{kg}{s}$
$\dot{m}_{GS}$	total mass of gases generated from solid due to gas solid reactions	$\frac{kg}{s}$
$\dot{m}_{GS,E}$	mass of gas generated in emulsion phase due to gas solid reactions	$\frac{kg}{s}$
$\dot{m}_{GS,E,j}$	mass of 'j'th gas generated in emulsion phase due to gas solid reactions	$\frac{kg}{s}$
$\dot{m}_{GS,j}$	total mass of gases due to gas solid reactions in 'j'	$\frac{kg}{s}$
Mj	Molecular weights	$\frac{kg}{kmol}$
M_j	molecular weight of component 'j'	$\frac{kg}{kmol}$
$\dot{m}_{out}$	mass flow rate out of the vapor phase	$\frac{kg}{s}$
$\dot{m}_{s,in}$	inlet mass flow rateof solids	$\frac{kg}{s}$
$\dot{m}_{S,out}$	outlet mass flow rate of solids	$\frac{kg}{s}$
$\dot{m}_{VM}$	inlet mass flow rate of volatile matter in coal particle	$\frac{kg}{s}$
nc	total number of components	-
ncs	number of components in solid phase	-
nr	number of reactions	-
nrs	number of reactions in solid phase	-
Nu	Nusselt number	-
O_{ij}	order of reaction	-
Pr	Prandtl number	-
P_{set}	reactor set pressure at any time ‘t’	Pa
P_V	vapor phase pressure at any time ‘t’	Pa
$q_{GB,E}$	convective heat transfer from the bubble phase to the emulsion phase	$\frac{kJ}{s}$
$q_{MGB,in}$	Energy ‘in’ by the inlet gases in the bubble phase at any time ‘t’	$\frac{kJ}{s}$
$q_{MGB,out}$	energy ‘out’ by the outlet gases exiting the bubble phase at any time ‘t’	$\frac{kJ}{s}$
$q_{MGE,B}$	energy transferred from by the emulsion phase to the bubble phase at any time ‘t’ (due to net flow)	$\frac{kJ}{s}$
$q_{MGE,in}$	energy ‘in’ by the inlet gases in the emulsion phase at any time ‘t’	$\frac{kJ}{s}$
$q_{MGE,out}$	energy out by the gases exiting the emulsion phase at any time ‘t’	$\frac{kJ}{s}$
$q_{MGS,E}$	energy transferred by mass generated due to gas solid reactions in the emulsion phase at any time ‘t’	$\frac{kJ}{s}$
$q_{MGV,out}$	energy ‘out’ by the outlet gases from the bubble phase at any time ‘t’	$\frac{kJ}{s}$

$q_{MSE,in}$	energy 'in' by the solids in the emulsion phase at any time 't'	$\frac{kJ}{s}$
$q_{MSE,out}$	energy 'out' by the solids exiting the emulsion phase at any time 't'	$\frac{kJ}{s}$
$q_{RGG,B}$	energy generated due to gas gas reactions in the emulsion phase at any time 't'	$\frac{kJ}{s}$
$q_{RGG,E}$	energy generated due to gas gas reactions in the emulsion phase at any time 't'	$\frac{kJ}{s}$
$q_{RGS,E}$	energy generated due to gas solid reactions in the emulsion phase at any time 't'	$\frac{kJ}{s}$
$q_{S,E}$	convective energy transfer from solids to the emulsion	$\frac{kJ}{s}$
R	gas constant	$\frac{J}{molK}$
Re	Reynolds number	-
$r_{GG,B,j}$	rate of generation of gas 'i' due to gas gas reactions in emulsion phase per unit volume	$\frac{kg}{m^3 s}$
$r_{GG,E,j}$	rate of generation of gas 'i' due to gas gas reactions in emulsion phase per unit volume	$\frac{kg}{m^3 s}$
$R_{ij,B}$	rate of 'i' reaction for the 'jth' component in bubble phase	$\frac{kmol}{m^3 s}$
$R_{ij,E}$	rate of 'i' reaction for the 'jth' component in emulsion phase	$\frac{kmol}{m^3 s}$
T_B	Temperature of bubble gases	K
$T_{B,in}$	inlet Temperature of emulsion gases	K
T_E	Temperature of emulsion gases	K
$T_{E,in}$	inlet Temperature of emulsion gases	K
T_s	temperature of the solids at any time 't'	K
$T_{S,E,in}$	inlet temperature of the solids at any time 't'	K
T_V	temperature of vapor phase at any time 't'	K
u_B	bubble rise velocity	$\frac{m}{s}$
U_G	superficial velocity of outlet gases	$\frac{m}{s}$
U_{MF}	minimum fluidisation velocity	$\frac{m}{s}$
V	volume of reactor (emulsion+bubble)	m^3
W_s	weight of solids in the reactor (emulsion) at any time t	kg
$x_{j,B}$	mole fraction of component j in bubble gas	-
$x_{j,E}$	mole fraction of component j in emulsion gas	-
$x_{j,V}$	mole fraction of component j in vapor gas	-
$y_{j,B}$	fraction of component 'j' in bubble phase	-
$y_{j,B,in}$	inlet fraction of component 'j' in bubble phase	-
$y_{j,E}$	fraction of component 'j' in emulsion phase	-
$y_{j,E,in}$	inlet fraction of component 'j' in emulsion phase	-
$y_{j,S}$	fraction of component 'j' in solid phase	-
$y_{j,S,in}$	inlet fraction of component 'j' in solid phase	-
$y_{j,V}$	fraction of component 'j' in vapor phase	-
$z_{i,ref}$	base stoichiometric coefficients	-

z_{ij}	stoichiometric coefficients	-
α	proportional constant for control valve	$\frac{kg}{sPa}$
ε_B	bubble voidage at any time 't'	-
ε_{MF}	voidage at minimum fluidisation conditions	-
ρ_{ash}	density of ash in solids	$\frac{kg}{m^3}$
ρ_G	density of gases in vapor phase at any time 't'	$\frac{kg}{m^3}$
ρ_{GB}	density of gases in bubble phase at any time 't'	$\frac{kg}{m^3}$
ρ_{GE}	density of gases in emulsion phase at any time 't'	$\frac{kg}{m^3}$
ρ_{GV}	density of gases in vapor phase at any time 't'	$\frac{kg}{m^3}$
$\rho_{j,B}$	density of 'jth' gas in bubble phase at any time 't'	$\frac{kg}{m^3}$
$\rho_{j,E}$	density of 'jth' gas in emulsion phase at any time 't'	$\frac{kg}{m^3}$
ρ_s	density of solids	$\frac{kg}{m^3}$
ρ_{VM}	density of volatile matter in solids	$\frac{kg}{m^3}$

References

1. British Petroleum. BP Statistical Review of World Energy. (2010). at <www.bp.com/productlanding.do?categoryId=6929&contentId=7044622S>

2. Reddy, V. S., Kaushik, S. C. & Panwar, N. L. Review on power generation scenario of India. *Renew. Sustain. Energy Rev.* **18,** 43–48 (2013).

3. Central Electricity Authority. Load Generation Balance Report 2014-15. (2014). at <http://www.cea.nic.in/reports/yearly/lgbr_report.pdf>

4. Yep, E. India's Widening Energy Deficit. *Wall Str. J.* (2011). at <http://blogs.wsj.com/indiarealtime/2011/03/09/indias-widening-energy-deficit/>

5. Central Electricity Regulatory Commision. Annual Report. (2011). at <http://www.cercind.gov.in/annual_report.html>

6. Kumar, U. & Jain, V. K. Time series models (Grey-Markov, Grey Model with rolling mechanism and singular spectrum analysis) to forecast energy consumption in India. *Energy* **35,** 1709–1716 (2010).

7. Khadse, A., Qayyumi, M., Mahajani, S. & Aghalayam, P. Underground coal gasification: A new clean coal utilization technique for India. *Energy* **32,** 2061–2071 (2007).

8. Steynberg, A. P. & Nel, H. G. Clean coal conversion options using Fischer–Tropsch technology. *Fuel* **83,** 765–770 (2004).

9. Rao, O. Coal gasification for sustainable development of energy sector in India. *Counc. Sci. Ind. Res. New Delhi* (1998). at <https://www.etde.org/etdeweb/details.jsp?osti_id=309054>

10. Schmal, M. Kinetics of coal gasification. *Ind. Eng. Chem. Process Des. Dev.* **21,** 256–266 (1982).

11. Gräbner, M. *Industrial Coal Gasification Technologies Covering Baseline and High-Ash Coal*. (Wiley-VCH Verlag GmbH & Co., 2015).

12. Collot, A.-G. Matching gasification technologies to coal properties. *Int. J. Coal Geol.* **65,** 191–212 (2006).

13. Kristiansen, A. *Understanding of coal gasification*. (IEA coal research, 1996).

14. André, F., Fernandes, N. & Lona, L. M. F. Fluidized-bed reactor modeling for polyethylene production. *J. Appl. Polym. Sci.* **81,** 321–332 (2001).

15. Gómez-Barea, A. & Leckner, B. Modeling of biomass gasification in fluidized bed. *Prog. Energy Combust. Sci.* **36,** 444–509 (2010).

16. Puig-Arnavat, M., Bruno, J. C. & Coronas, A. Review and analysis of biomass gasification models. *Renew. Sustain. Energy Rev.* **14,** 2841–2851 (2010).

17. Loha, C., Gu, S., De Wilde, J., Mahanta, P. & Chatterjee, P. K. Advances in mathematical modeling of fluidized bed gasification. *Renew. Sustain. Energy Rev.* **40,** 688–715 (2014).

18. Chavan, P. *et al.* Development of data-driven models for fluidized-bed coal gasification process. *Fuel* **93,** 44–51 (2012).

19. Yu, L., Lu, J., Zhang, X. & Zhang, S. Numerical simulation of the bubbling fluidized bed coal gasification by the kinetic theory of granular flow (KTGF). *Fuel* **86,** 722–734 (2007).

20. Wang, X., Jin, B. & Zhong, W. Three-dimensional simulation of fluidized bed coal gasification. *Chem. Eng. Process. Process Intensif.* **48,** 695–705 (2009).

21. Armstrong, L., Gu, S. & Luo, K. H. Parametric Study of Gasification Processes in a BFB Coal Gasifier. *Ind. Eng. Chem. Res.* **50,** 5959–5974 (2011).

22. Armstrong, L. M., Gu, S., Luo, K. H. & Mahanta, P. Multifluid Modeling of the Desulfurization Process within a Bubbling Fluidized Bed Coal Gasifier. *AIChE J.* **59,** 1952–1963 (2013).

23. Bacon, D., Downie, J., Hsu, J. & Peters, J. *Fundamentals of thermochemical biomass conversion*. (Elsevier, 1982).

24. Kersten, S., Prins, W., Van der Drift, A. & Van Swaaij, W. Interpretation of biomass gasification by "'quasi'"-equilibrium models. in *Twelfth Eur. Conf. Biomass Energy, Ind. Clim. Prot.* 556–559 (2002).

25. Li, X., Grace, J. R., Watkinson, A. P., Lim, C. J. & Ergüdenler, A. Equilibrium modeling of gasification: a free energy minimization approach and its application to a circulating fluidized bed coal gasifier. *Fuel* **80,** 195–207 (2001).

26. Jarungthammachote, S. & Dutta, a. Thermodynamic equilibrium model and second law analysis of a downdraft waste gasifier. *Energy* **32,** 1660–1669 (2007).

27. Zainal, Z. A., Ali, R., Lean, C. H. & Seetharamu, K. N. Prediction of performance of a downdraft gasifier using equilibrium modeling for different biomass materials. *Energy Convers. Manag.* **42,** 1499–1515 (2001).

28. Loha, C., Chattopadhyay, H. & Chatterjee, P. K. Thermodynamic analysis of hydrogen rich synthetic gas generation from fluidized bed gasification of rice husk. *Energy* **36,** 4063–4071 (2011).

29. Fryda, L., Panopoulos, K. D., Karl, J. & Kakaras, E. Exergetic analysis of solid oxide fuel cell and biomass gasification integration with heat pipes. *Energy* **33,** 292–299 (2008).

30. Schuster, G., Löffler, G., Weigl, K. & Hofbauer, H. Biomass steam gasification--an extensive parametric modeling study. *Bioresour. Technol.* **77,** 71–79 (2001).

31. Grace, J. R., Li, X. & Lim, C. J. Equilibrium modelling of catalytic steam reforming of methane in membrane reactors with oxygen addition. *Catal. today* **64,** 141–149 (2001).

32. Yan, H., Heidenreich, C. & Zhang, D. Mathematical modelling of a bubbling fluidised-bed coal gasifier and the significance of "net flow." *Fuel* **77,** 1067–1079 (1998).

33. Goyal, A., Pushpavanam, S. & Voolapalli, R. K. Modeling and simulation of co-gasification of coal and petcoke in a bubbling fluidized bed coal gasifier. *Fuel Process. Technol.* **91,** 1296–1307 (2010).

34. Chavan, Datta, S., Saha, S., Sahu, G. & Sharma, T. Influence of high ash Indian coals in fluidized bed gasification under different operating conditions. *Solid Fuel Chem.* **46,** 108–113 (2012).

35. Harshe, Y. M., Utikar, R. P. & Ranade, V. V. A computational model for predicting particle size distribution and performance of fluidized bed polypropylene reactor. *Chem. Eng. Sci.* **59,** 5145–5156 (2004).

36. Gautam, G., Adhikari, S. & Bhavnani, S. Estimation of Biomass Synthesis Gas Composition using Equilibrium Modeling. *Energy & Fuels* **24,** 2692–2698 (2010).

37. Shabbar, S. & Janajreh, I. Thermodynamic equilibrium analysis of coal gasification using Gibbs energy minimization method. *Energy Convers. Manag.* **65,** 755–763 (2013).

38. Renganathan, T., Yadav, M. V., Pushpavanam, S., Voolapalli, R. K. & Cho, Y. S. CO2 utilization for gasification of carbonaceous feedstocks: A thermodynamic analysis. *Chem. Eng. Sci.* **83,** 159–170 (2012).

39. Khan, A. a., De Jong, W., Gort, D. R. & Spliethoff, H. A fluidized bed biomass combustion model with discretized population balance. 1. Sensitivity analysis. *Energy and Fuels* **21,** 2346–2356 (2007).

40. Ross, D., Yan, H., Zhong, Z. & Zhang, D. A non-isothermal model of a bubbling fluidised-bed coal gasifier. *Fuel* **84,** 1469–1481 (2005).

41. Kaushal, P., Abedi, J. & Mahinpey, N. A comprehensive mathematical model for biomass gasification in a bubbling fluidized bed reactor. *Fuel* **89,** 3650–3661 (2010).

42. Merrick, D. Mathematical models of the thermal decomposition of coal: 1. The evolution of volatile matter. *Fuel* **62,** 534–539 (1983).

43. Mathworks. http://www.mathworks.in/help/matlab/ref/ode15s.html. (2013).

44. Ranade, V. V. & Gupta, D. F. *Computational modeling of pulverized coal fired boilers*. (CRC Press, 2015).

45. Kim, B. *et al.* Devolatilization and Cracking Characteristics of Australian Lumpy Coals. **50,** 514–522 (2008).

46. Huang, H.-J. & Ramaswamy, S. Modeling biomass gasification using thermodynamic equilibrium approach. *Appl. Biochem. Biotechnol.* **154,** 14–25 (2009).

47. Syed, S., Janajreh, I. & Ghenai, C. Thermodynamics Equilibrium Analysis within the Entrained Flow Gasifier Environment. *Int. J. Therm. Environ. Eng.* **4,** 47–54 (2011).

48. Loha, C., Chatterjee, P. K. & Chattopadhyay, H. Performance of fluidized bed steam gasification of biomass – Modeling and experiment. *Energy Convers. Manag.* **52,** 1583–1588 (2011).

49. Barman, N. S., Ghosh, S. & De, S. Gasification of biomass in a fixed bed downdraft gasifier--a realistic model including tar. *Bioresour. Technol.* **107,** 505–11 (2012).

50. Janajreh, I., Raza, S. S. & Valmundsson, A. S. Plasma gasification process: Modeling, simulation and comparison with conventional air gasification. *Energy Convers. Manag.* **65,** 801–809 (2013).

51. Hamel, S. & Krumm, W. Mathematical modelling and simulation of bubbling fluidised bed gasifiers. *Powder Technol.* **120,** 105–112 (2001).

52. Chejne, F. & Hernandez, J. P. Modelling and simulation of coal gasication process in fluidised bed. *Fuel* **81,** 1687–1702 (2002).

53. Chejne, F., Lopera, E. & Londoño, C. A. Modelling and simulation of a coal gasification process in pressurized fluidized bed. *Fuel* **90,** 399–411 (2011).

54. Kunii, D. & Levenspiel, O. *Fluidization Engineering*. (Butterworth-Heinemann, Boston, MA., 1991).

55. Weimer, A. W. & Clough, D. E. Modeling a low pressure steam-oxygen fluidized bed coal gasifying reactor. *Chem. Eng. Sci.* (1981). doi:10.1016/0009-2509(81)80144-3

List of Figures

List of Tables

APPENDIX A

Overall mass balance across the emulsion phase

$$\dot{\mathbf{m}}_{\mathbf{GE,out}} + \dot{\mathbf{m}}_{\mathbf{GE,B}} = \dot{\mathbf{m}}_{\mathbf{GE,in}} + \dot{\mathbf{m}}_{\mathbf{GS,E}} + \dot{\mathbf{m}}_{\mathbf{VM}} \quad (1)$$

$$\dot{m}_{GE,in} = A(1-\varepsilon_B)U_{mf}\rho_{GE} \quad (2)$$

$$\dot{m}_{GE,out} = A(1-\varepsilon_B)U_{mf}\rho_{GE} \quad (3)$$

$$\dot{m}_{GE,in} = \dot{m}_{GE,out} \quad (4)$$

$$\dot{m}_{GB,in} = \dot{m}_{G,in} - \dot{m}_{GE,in} \quad (5)$$

$$\rho_{GE} = \frac{P_V M_{avg,E}}{RT_E} \quad (7)$$

$$\rho_{GB} = \frac{P_V M_{avg,B}}{RT_B} \quad (8)$$

$$M_{avg,E} = \sum_{j=nc-ncs}^{nc} x_{j,E} M_j \quad (9)$$

$$x_{j,E} = \frac{\frac{y_{j,E}}{M_{j,E}}}{\sum_{j=nc-ncs}^{nc} \frac{y_{j,E}}{M_{j,E}}} \quad (10)$$

$$M_{avg,B} = \sum_{j=nc-ncs}^{nc} x_{j,B} M_j \quad (11)$$

$$x_{j,B} = \frac{\frac{y_{j,B}}{M_{j,B}}}{\sum_{j=nc-ncs}^{nc} \frac{y_{j,B}}{M_{j,B}}} \quad (12)$$

$$\dot{m}_{GE,B} = \dot{m}_{GS,E} + \dot{m}_{VM} \quad (14)$$

$$\dot{m}_{GS,E} = \sum_{i=1}^{nrs} \sum_{j=nc-ncs}^{nc} R_{ij,E} M_j \quad (15)$$

Overall steady state mass balance across the bubble phase

$$0 = \dot{m}_{GB,in} - \dot{m}_{GB,out} - \sum_{j=ncs+1}^{nc} k_{be}^{j} \rho_G (y_{j.B} - y_{j,E}) V \epsilon_B + \dot{m}_{GE,B} \quad (16)$$

$$\dot{m}_{GB,out} = \dot{m}_{GB,in} + \dot{m}_{GE,B} \quad (17)$$

$$\rho_G = \frac{\rho_{GE} \dot{m}_{GE,out} + \rho_{GB} \dot{m}_{GB,out}}{\dot{m}_{GE,out} + \dot{m}_{GB,out}} \quad (18)$$

Superficial velocity of the total mass of gas out

$$U_G = \frac{\dot{m}_{GE,out} + \dot{m}_{GB,out}}{A \rho_G} \quad (19)$$

Overall mass balance for solids

$$\frac{dW_S}{dt} = \dot{m}_{s,in} - \dot{m}_{s,out} - \dot{m}_{GS} \quad (20)$$

$$\dot{m}_{s,out} = \varphi \dot{m}_{s,in} \quad (21)$$

$$\dot{m}_{GS} = \sum_{i=1}^{nrs} \sum_{j=1}^{ncs} R_{ij,E} M_j \quad (22)$$

Density of solids

$$\rho_s = \dot{m}_C \rho_c + \dot{m}_{ash} \rho_{ash} + \dot{m}_{VM} \rho_{VM} \quad (23)$$

Solids component balance

$$\frac{d}{dt}(W_s y_{j,S}) = \dot{m}_{S,in} y_{j,S,in} - \dot{m}_{S,out} y_{j,S} - \dot{m}_{GS,j} \quad (24)$$

$$\dot{m}_{GS,j} = \sum_{i=1}^{nrs} R_{ij,E} M_j \quad (25)$$

Component mass balance for emulsion phase gas

$$\frac{d}{dt}\left(\rho_{GE} V(1-\varepsilon_B)\varepsilon_{mf} y_{j,E}\right) = \dot{m}_{GE,in} y_{j,E,in} - \dot{m}_{GE,out} y_{j,E} + \dot{m}_{GS,E,j} + r_{GG,E,j} V(1-\varepsilon_B)\epsilon_{mf} + k_{be}^{j} \rho_G \left(y_{j.B} - y_{j,E}\right) V \epsilon_B - \dot{m}_{GE,B} y_{j,E} \quad (26)$$

$$r_{GG,E,j} = \sum_{i=nrs+1}^{nr} R_{ij,E} M_j \quad (27)$$

$$\dot{m}_{GS,E,j} = \sum_{i=1}^{nrs} R_{ij,E} M_j \quad (28)$$

Component mass balance for bubble phase gas

$$\frac{d}{dt}\left(\rho_{GB} V \epsilon_B y_{j,B}\right) = \dot{m}_{GB,in} y_{j,B,in} - \dot{m}_{GB,out} y_{j,B} + r_{GG,B,j} V \varepsilon_B - k_{be}^{j} \rho_G \left(y_{j.B} - y_{j,E}\right) V \epsilon_B + \dot{m}_{GE,B} y_{j,E} \quad (29)$$

$$r_{GG,B,j} = \sum_{i=nrs+1}^{nr} R_{ij,B} M_j \quad (30)$$

Overall mass balance in the vapor phase

$$\frac{d}{dt}\left(\rho_{GV} \quad A(H_{max} - H) y_{j,v} \quad\right) = \dot{m}_{GE,out} y_{j,E} + \dot{m}_{GB,out} y_{j,B} - \dot{m}_{out} \quad y_{j,v} \quad + r_{GG,V,j} \quad V_v \quad (31)$$

$$\rho_{GV} = \frac{P_V M_{avg,V}}{R T_V} \quad (32)$$

$$M_{avg,V} = \sum_{j=nc-ncs}^{nc} x_{j,V} M_j \quad (33)$$

$$x_{j,V} = \frac{\frac{y_{j,V}}{M_{j,V}}}{\sum_{j=nc-ncs}^{nc} \frac{y_{j,V}}{M_{j,V}}} \quad (34)$$

$$\dot{m}_{out} = \alpha(P - P_{set}) \quad (35)$$

Energy Balance Equations

Overall energy balance for solid phase

$$\frac{d}{dt}\left(W_s C_{P,S} T_S\right) = \dot{q}_{MSE,in} - \dot{q}_{MSE,out} + \dot{q}_{RGS,E} - \dot{q}_{MGS,E} - \dot{q}_{S,E} \quad (37)$$

$$\dot{q}_{MSE,in} = \dot{m}_{s,in} c_{P,S}\left(T_{S,in} - T_{ref}\right) \quad (38)$$

$$\dot{q}_{MSE,out} = \dot{m}_{s,out} c_{P,S}(T_S - T_{ref}) \quad (39)$$

$$\dot{q}_{RGS,E} = \sum_{i=1}^{nrs} \sum_{j=1}^{ncs} R_{ij,E}\, M_j (-\Delta H)_i \quad (40)$$

$$\dot{q}_{S,E} = h_{GE-S} A_S (T_S - T_E) \quad (41)$$

$$\dot{q}_{MGS,E} = \dot{m}_{GS,E} C_{p,E,eff} (T_S - T_E) \quad (42)$$

$$C_{p,E,eff} = \sum_{j=nc-ncs}^{nc} y_{j,E} C_{p,E,j} \quad (43)$$

Overall emulsion phase energy balance equation

$$\frac{d}{dt}\left(V(1-\varepsilon_B)\epsilon_{mf} T_E \sum_{j=nc-ncs}^{nc} \rho_{GE} y_{j,E} C_{p,E,j}\right) = \dot{q}_{MGE,in} - \dot{q}_{MGE,out} + \dot{q}_{RGG,E} + \dot{q}_{MGS,E} - \dot{q}_{MGE,B} + \dot{q}_{S,E} + \dot{q}_{GB,E} \quad (44)$$

$$\dot{q}_{MGE,in} = \dot{m}_{GE,in} C_{p,E,in,eff} \left(T_{E,in} - T_{ref}\right) \quad (45)$$

$$C_{p,E,in,eff} = \sum_{j=nc-ncs}^{nc} y_{j,E,in} C_{p,E_j} \quad (46)$$

$$\dot{q}_{MGE,out} = \dot{m}_{GE,out} C_{p,E,eff} (T_E - T_{ref}) \quad (47)$$

$$\dot{q}_{RGG,E} = V(1 - \varepsilon_B) \epsilon_{mf} \sum_{i=nr-nrs}^{nr} \sum_{j=nc-ncs}^{nc} R_{ij,E} M_j (-\Delta H_i) \quad (48)$$

$$\dot{q}_{MGE,B} = \dot{m}_{GE,B} C_{p,E,eff} (T_E - T_{ref}) \quad (49)$$

$$\dot{q}_{GB,E} = h_{GE-B} V(\epsilon_B)(T_B - T_E) \quad (50)$$

Energy transfer in bubble phase

$$\frac{d}{dt}\left(V \varepsilon_B T_B \sum_{j=nc-ncs}^{nc} \rho_{GB} y_{j,B} C_{p,B,j}\right) = \dot{q}_{MGB,in} - \dot{q}_{MGB,out} + \dot{q}_{RGG,B} + \dot{q}_{MGE,B} - \dot{q}_{GB,E} \quad (51)$$

$$\dot{q}_{MGB,in} = \dot{m}_{GB,in} C_{p,B,in,eff} \left(T_{B,in} - T_{ref}\right) \quad (52)$$

$$C_{p,B,in,eff} = \sum_{j=nc-ncs}^{nc} y_{j,B,in} C_{p,B_j} \quad (53)$$

$$\dot{q}_{MGB,out} = \dot{m}_{GB,out} C_{p,B,eff} (T_B - T_{ref}) \quad (54)$$

$$C_{p,B,eff} = \sum_{j=nc-ncs}^{nc} y_{j,B} C_{p,B_j} \quad (55)$$

$$\dot{q}_{RGG,B} = V \epsilon_B \sum_{i=nr-nrs}^{nr} \sum_{j=nc-ncs}^{nc} R_{ij,B} M_j (-\Delta H_i) \quad (56)$$

Overall vapor phase energy balance equations

$$\frac{d}{dt}\left(\rho_{GV} \quad A(H_{max} - H) T_V \quad \sum_{i=nc-ncs}^{nc} C_{P,V,j} \quad y_{j,V} \quad\right) = \dot{q}_{MGE,out} + \dot{q}_{MGB,out} + \dot{q}_{RGG,V} \quad - \dot{q}_{MGV,out} \quad (57)$$

$$\dot{q}_{MGV,out}{}^{z} = \dot{m}_{out}{}^{z} C_{p,V,eff}{}^{z} (T_V{}^{z} - T_{ref}) \quad (58)$$

$$\dot{q}_{RGG,B}{}^{k} = V_V \sum_{i=nr-nrs}^{nr} \sum_{j=nc-ncs}^{nc} R_{ij,V}{}^{z} M_j{}^{z} (-\Delta H_i)^{z} \quad (59)$$

$$C_{p,V,eff}{}^{z} = \sum_{j=nc-ncs}^{nc} y_{j,V}{}^{z} C_{p,V,j}{}^{z} \quad (60)$$

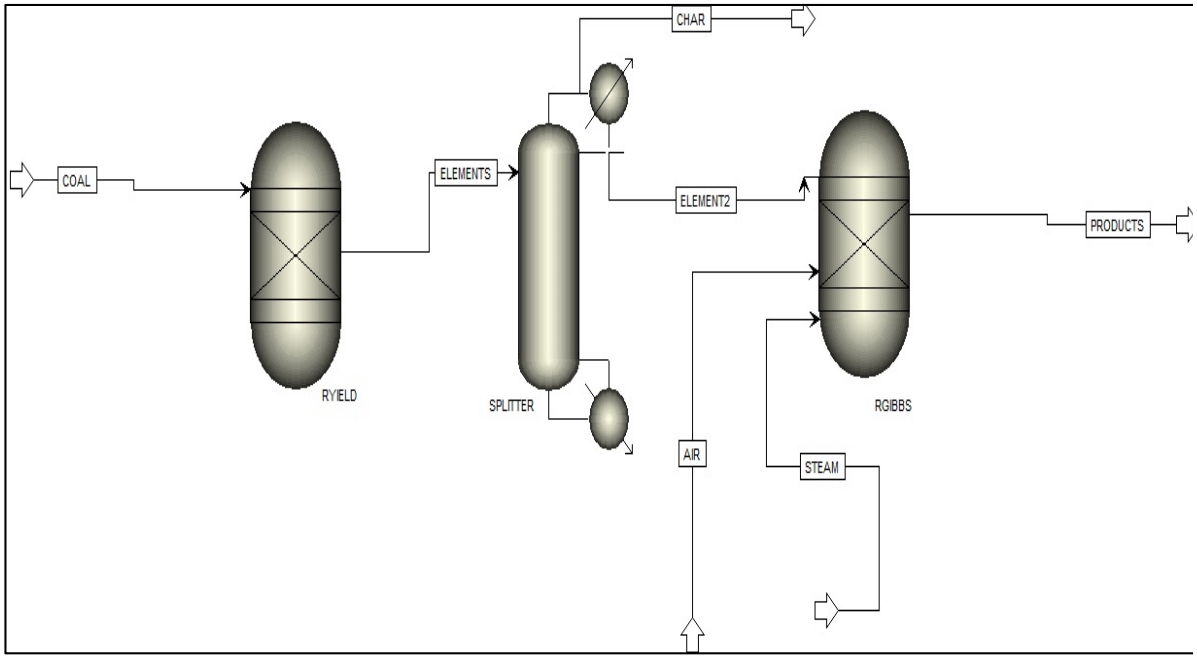

Figure 1: Aspen Plus Model Flow sheet

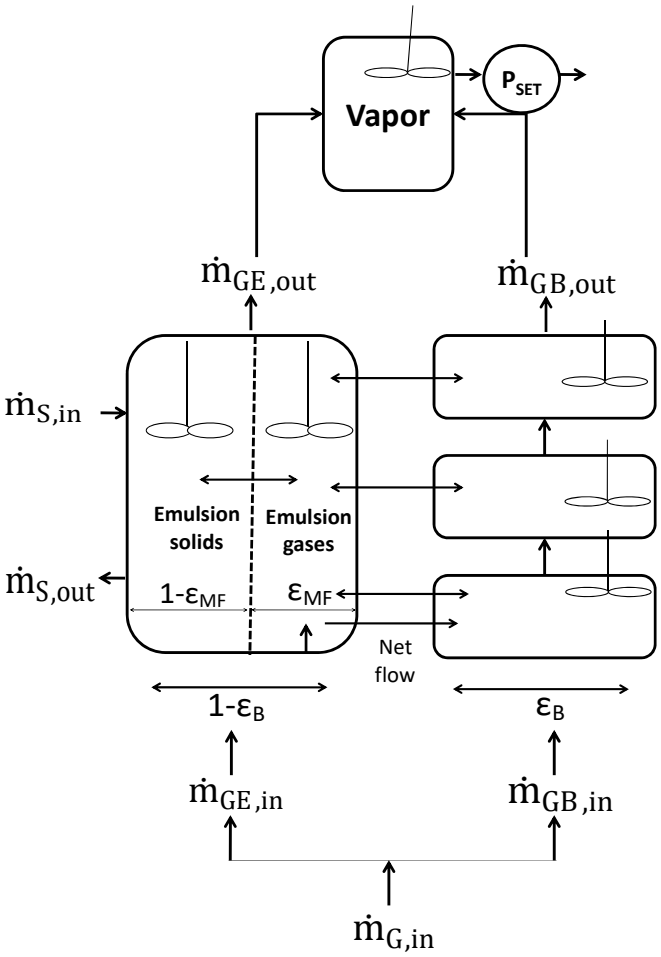

Figure 2: CRE model for a fluidized bed gasifier reactor

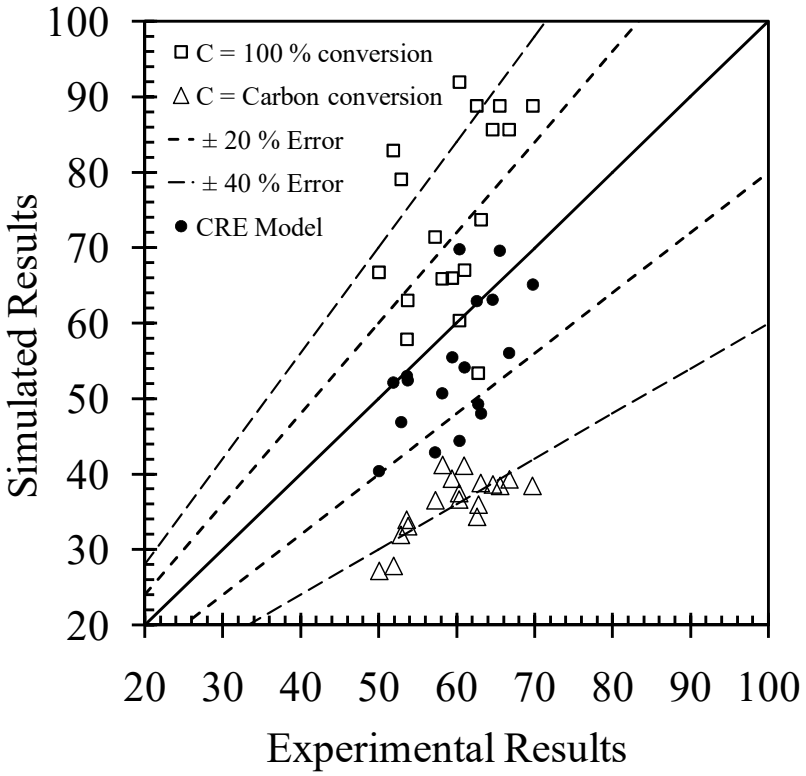

Figure 3a: Parity plot comparing the simulation results of 18 experimental data with Rajmahal coal for CGE

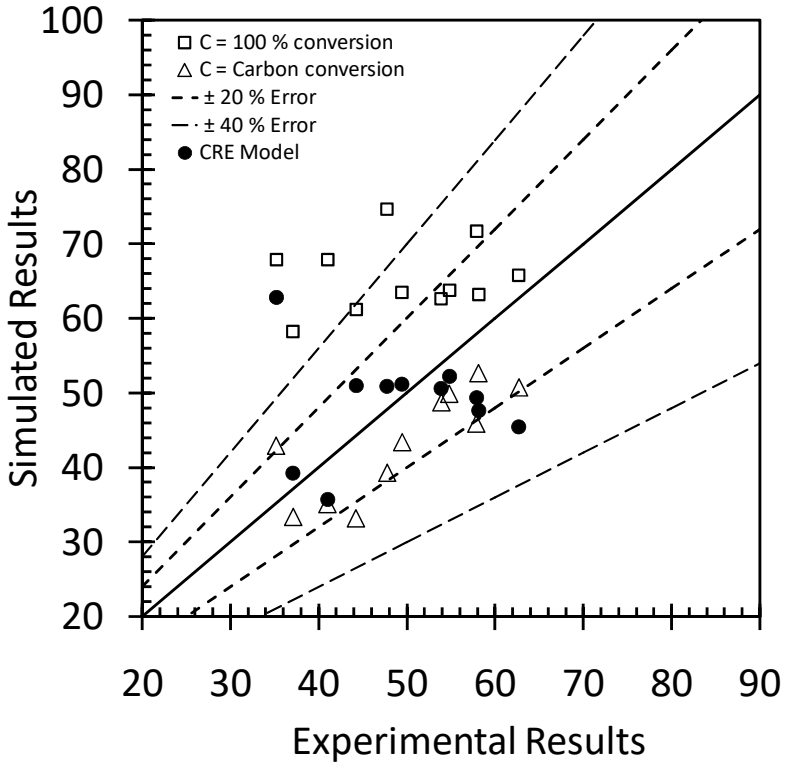

Figure 3b: Parity plot comparing the simulation results of 11 experimental data with North Karanpura (NK) coal for CGE

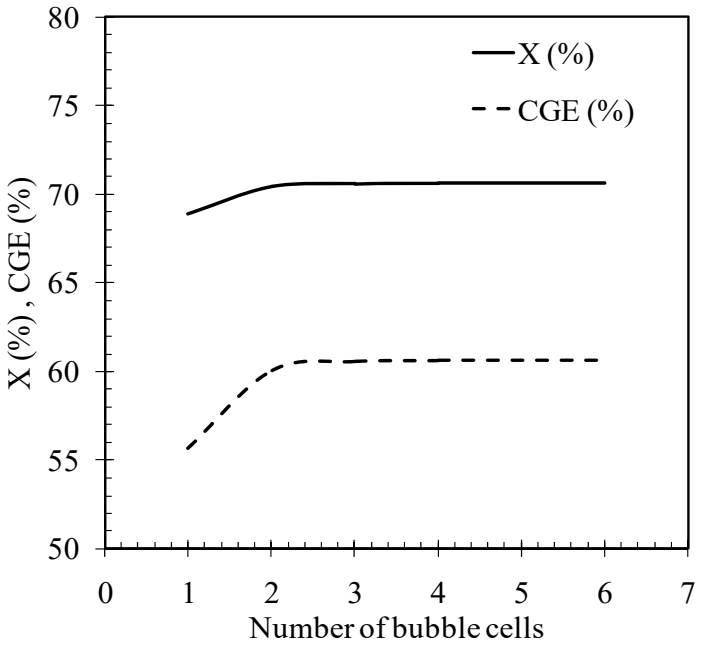

Figure 4a: Effect of bubble mixing cells on CGE and X

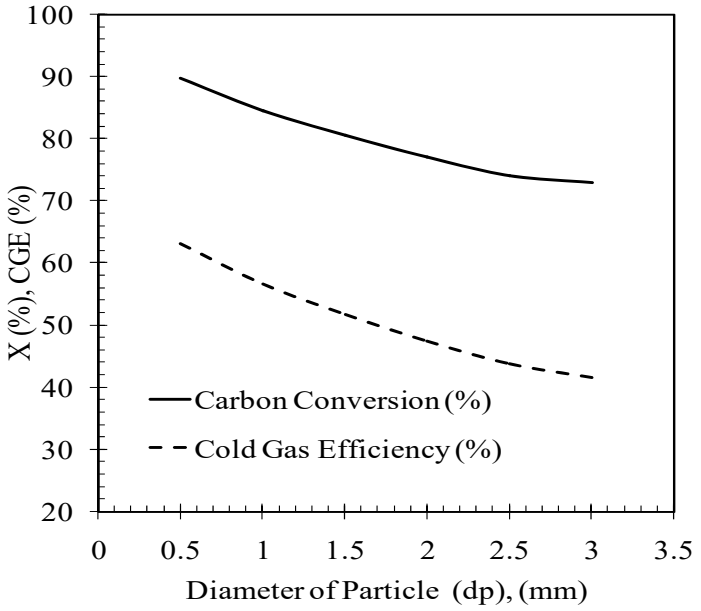

Figure 4b: Variation in CGE and X with d_p

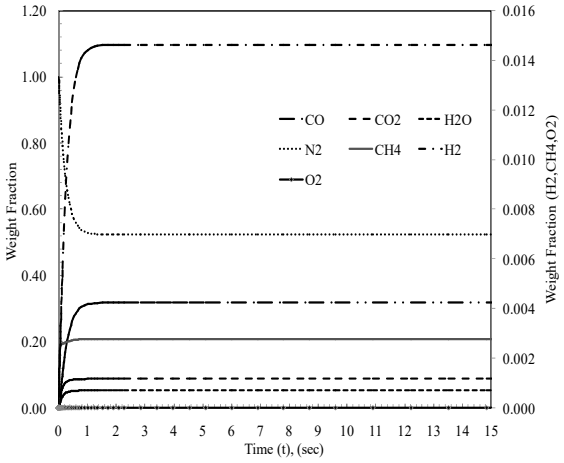

Figure 5a: Typical profile of gaseous species in the emulsion phase

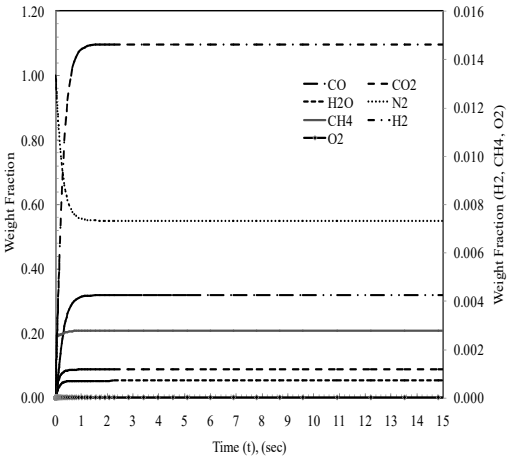

Figure 5b: Typical profile of gaseous species in the bubble phases

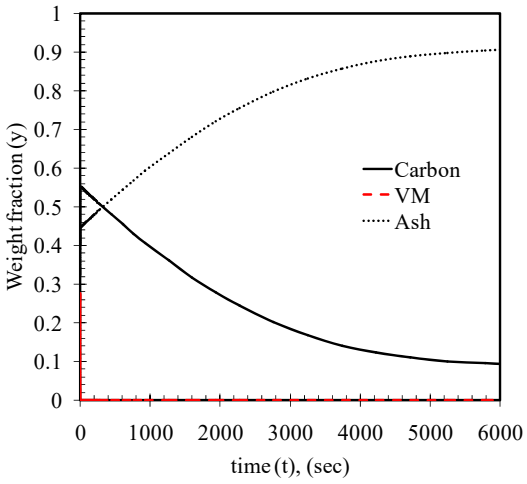

Figure 5c: Typical profile of the solids species in the solids phase

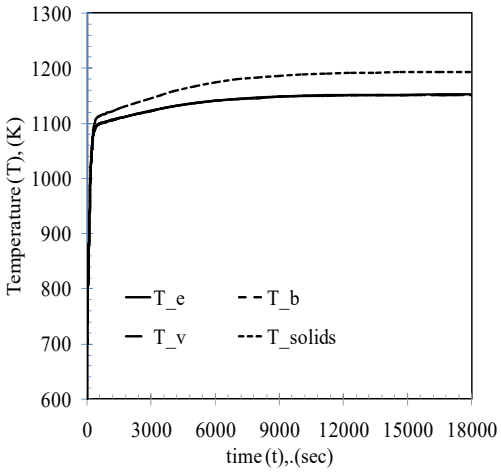

Figure 5d: Temperature profile for the emulsion, solid, bubble and vapour phase

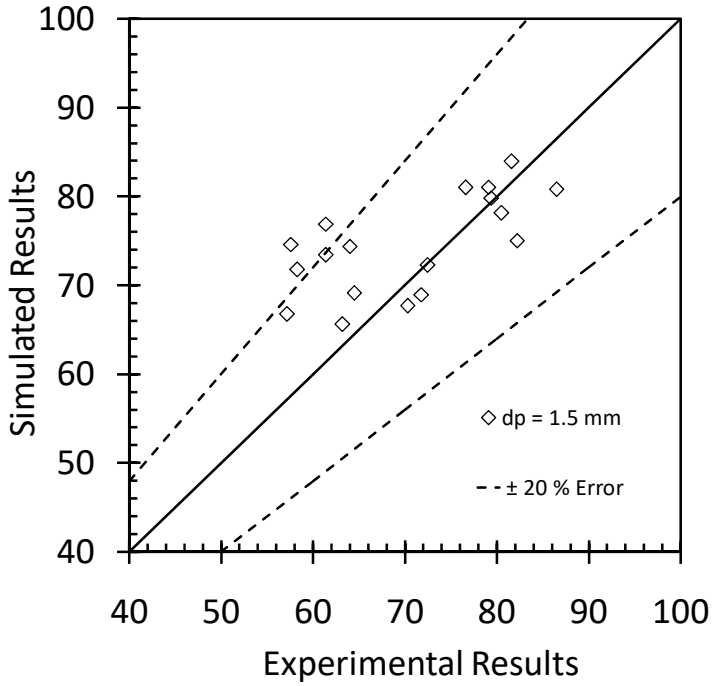

Figure 6a: Parity plot comparing the simulation results of 18 experimental data with Rajmahal coal for carbon conversion

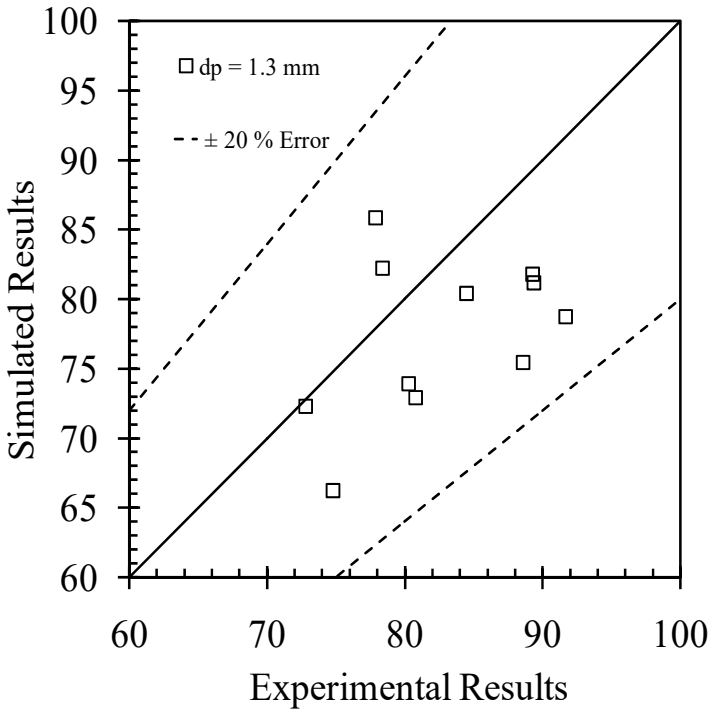

Figure 6b: Parity plot comparing the simulation results of 11 experimental data of North Karanpura coal (NK) for carbon conversion

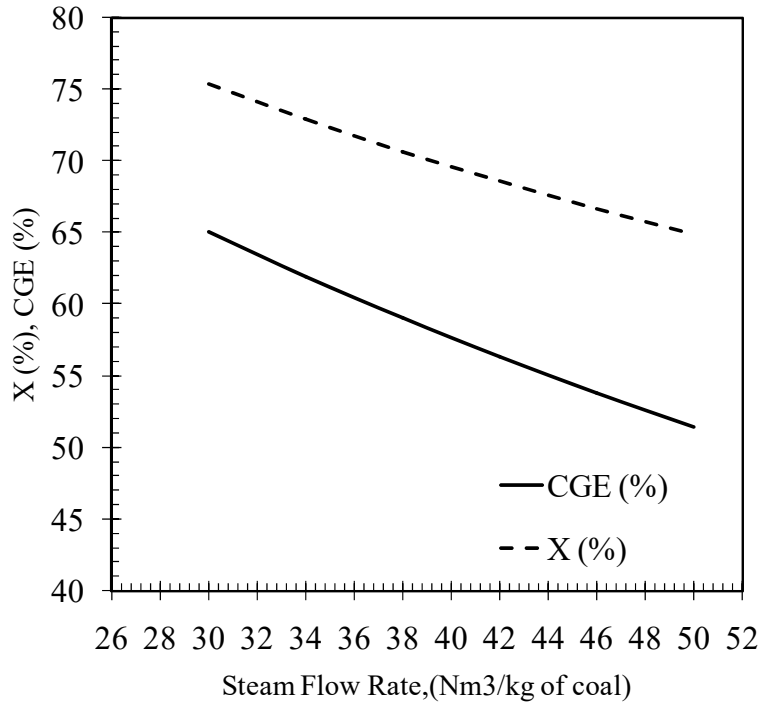

Figure 7a: Influence of coal feed rate to the carbon conversion and the cold gas efficiency

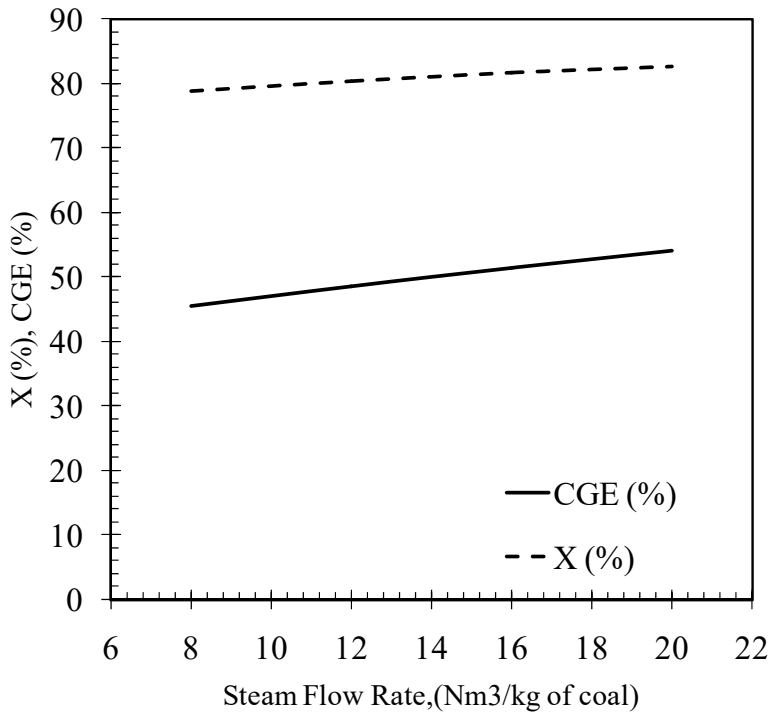

Figure 7b: Influence of steam feed rate to the carbon conversion and the cold gas efficiency

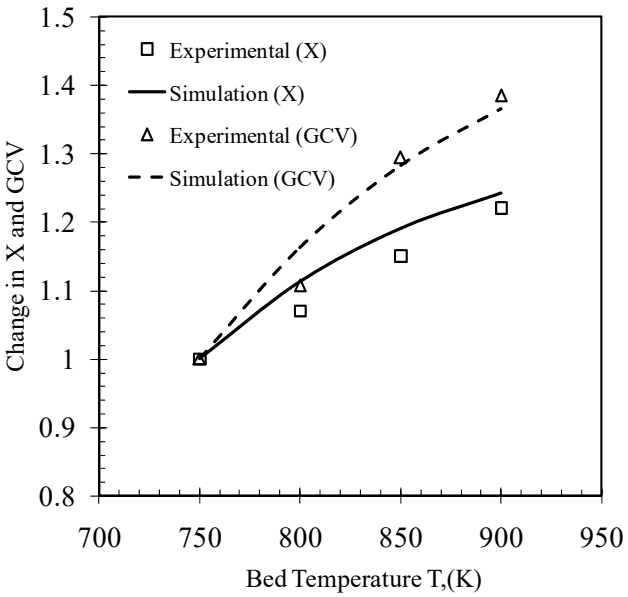

Figure 7c: Influence of bed temperature to the carbon conversion and the GCV

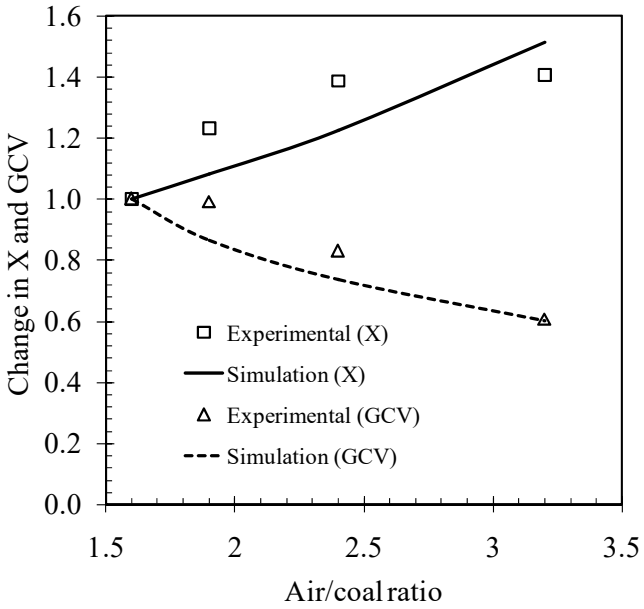

Figure 7d: Influence of air/coal ratio to the carbon conversion and the GCV

Table 1a: Review of Thermodynamic models

Reference	Feed	Type of thermodynamic model	Compared with experimental data	Reactor Type	Comments
[30]	Biomass	Non stoichiometric	No	No	Application of dual bed biomass FBG Steam gasification
[27]	Biomass	stoichiometric	Yes	Downdraft gasifier	Compared Calorific value with experimental data
[46]	Biomass	Stoichiometric	Yes	Downdraft	Modified the equilibrium constants to find better match with experimental data
[36]	Biomass	Stoichiometric	Yes	Downdraft	Proposed a correlation to predict CO, CO2, based on the elemental analysis
[47]	Biomass	Non Stoichiometric	No	No	Application for entrained bed gasifier
[48]	Biomass	Stoichiometric	Yes	BFBG	Steam Gasification of Rice husk Modified the equilibrium constants to match the experimental data
[49]	Biomass	Stoichiometric	Yes	Downdraft	Modified the equilibrium constants to find better match with experimental data Also included tar in the model
[50]	Biomass	Non Stoichiometric	No	No	Plasma gasification and air gasification CGE comparison done
[37]	Coal	Non stoichiometric	No	NA	Input of exhaustive set of 44 species
This work	Coal	Non stoichiometric	Yes	BFBG	Experimental conditions as reported for 29 experimental data points of BFBG

Table 1b: Review of CRE Models

No.	Reference	Type of Model	Comments
1	[32]	1D steady state (two phase theory with net flow)	(a) Compared simulation results with experimental data of a commercial gasifier (Certain critical parameters viz carbon conversion, coal feed rate not reported) (b) Compared results with and without netflow assumption
2	[51]	1D steady state (two phase theory)	(a) Developed a cell model wherein four different set of experimental data at different scale (height of gasifier 3.7 m , 4 m, 14.7 m , 23 m) to validate the results of their model
3	[52]	1D steady state (two phase theory)	(a) Plugged in a model to account for the particle size distribution (b) Validated their model results with experiments conducted in their own group
4	[40]	1D steady state (two phase theory)	(a) Included energy balance equations for the phases in the model as reported in [32] (b) Predicted solids temperature higher than gas temperature leading to higher carbon conversion
7	[33]	1D steady state (two phase theory)	(a) Used the same model as reported in [40] to study co-gasification of petcoke and coal (b) Effect of feed inlet position on gasifier performance has been shown
9	[53]	1D steady state (two phase theory)	(a) Included correlations to study the effects of pressure in the previous model [53] on hydrodynamics and gasifier performance

Table 2: List of correlations used in this model

Sr. No.	Parameter	Correlation	Reference
1.	Diameter of rising bubble, d_B	$d_b = \left(\frac{(U_g - U_{mf})^{\frac{1}{2}} (h + h_o)^{\frac{3}{4}} g^{-\frac{1}{4}}}{100} \right)$	54
2.	Bubble rise velocity , u_B	$u_B = u_g - u_{mf} + 0.711\sqrt{g d_B}$	54
3.	Mass transfer coefficient, k_{BE}	$k_{BE} = 2\left(\frac{u_{mf}}{d_B}\right) + 12\left(\frac{D_g^{0.5} {\varepsilon_{mf}}^{0.5} {u_B}^{0.5}}{(\pi {d_B}^3)^{0.5}}\right)$	54
4.	Heat transfer coefficient bubble-cloud ,h_{BC}	$h_{BC} = 4.5\left(\frac{u_{mf}\rho_g C_{p_g}}{d_B}\right) + 10.4\left(\frac{k_g \rho_g C_{p_g}}{{d_B}^{2.5}}\right)^{0.5}$	54
5.	Heat transfer coefficient cloud emulsion, h_{CE}	$h_{CE} = 6.78\left(k_g \rho_g C_{p_g}\right)^{0.5}\left(\frac{\varepsilon_{mf} u_B}{{d_B}^3}\right)^{0.5}$	54
6.	Heat transfer bubble emulsion, h_{BE}	$\frac{1}{h_{GE-B}} = \frac{1}{h_{BC}} + \frac{1}{h_{CE}}$	54
7.	Volume fraction of bubbles, ε_B	$\varepsilon_B = \frac{U_G - U_{MF}}{u_B}$ $\varepsilon_B = 1 - \frac{1}{f_{b,ex}}$ $f_{b,ex} = 1 + \frac{(14.31(u_0 - u_{mf})^{0.738} d_p^{1.006} \rho_s^{0.376})}{(\rho_g^{0.126} u_{mf}^{0.937})}$	54, 52
8.	Minimum fluidization velocity, u_{mf}	Ergun equation	54
9.	Heat transfer solid emulsion, h_{GE-s}	$h_{ge-s}^i = \frac{Nuk_g}{d_P}$	54
10	Nusselt Number, Nu	$Nu = 0.4\left(\frac{Re}{\varepsilon_e}\right)^{\frac{2}{3}} Pr^{\frac{1}{3}}$	54
11	Reynolds Number, Re	$Re = \frac{\rho v d_p}{\mu}$	54
12	Prandtl Number, Pr	$Pr = \frac{C_{p,j}\mu}{k_g}$	54

Table 3 Reaction rate expression for the chemical reactions

No.	Rate expression	Pre exponential factor (ko)	Activation Energy (J/kmol)	Heat of reaction (J/kmol)	References
R1	Instantaneous	NA	NA	NA	[55]
R2	$R2 = k_2C_{O2}$	1.55E07 (1/s)	1.247E08	350E06	[55]
R3	$R3 = k3C_{H20}$	3.42Tc (1/s)	1.297sE08	-131.4E06	[51]
R4	$R4 = k4C_{CO2}$	342Tc (1/s)	1.279E08	-172.5E06	[22]
R5	$R5 = k5C_{H2}$	0.00342Tc (1/s)	1.297E08	74.9E06	[22]
R5’	$R_5' = k_5'C_{CO}C_{H20}$	2.978E12 (m3/kmol/s)	3.690E08	4.2E07	[55]
R6’	$R_6' = k_6'C_{CO2}C_{H2}$	7.145E14 (m3/kmol/s)	3.983E08	-4.2E07	[55]
R5	$R_5 = k_5C_{CO}C_{H20}$	$30\varepsilon_{mf}$ (m3/kmol/s)	6.027E07	4.2E07	[55]
R6	$R_6 = k_6C_{CO2}C_{H2}$	$1362\ \varepsilon_{mf}$ (m3/kmol/s)	9.492E07	-4.2E07	[55]
R7	$R_7 = k_7C_{CO}C_{O2}$	3.09E08 (m3/kmol/s)	9.976E07	2.83E08	[55]
R8	$R_8 = k_8C_{H2}^{1.5}C_{O2}$	$1.631E09T^{1.5}$ (m3/kmol/s)	3420R	2.41E08	[51]
R9	$R_9 = k_9T^{-1}C_{CH4}C_{O2}$	3.552E14 (m3/kmol/s)	15700R	5.194E08	[51]

In the rate expressions $*k_i = k_oe^{-(E/RT)}$

R5’, R6’ = reactions in emulsion phase

R5,R6 = reactions in bubble phase